

Electrodynamic response of Sr₂RuO₄

R. J. Ormeno, M. A. Hein,* T. L. Barraclough, A. Sibley, and C. E. Gough

School of Physics and Astronomy, The University of Birmingham, Edgbaston, Birmingham B15 2TT, United Kingdom

Z. Q. Mao, S. Nishizaki, and Y. Maeno

Department of Physics, Kyoto University, Kyoto 606-01, Japan

and CREST, Japan Science and Technology Corporation, Japan

(Received 19 June 2006; published 28 September 2006)

The surface impedance $Z_s = R_s + iX_s$ of a number of Sr₂RuO₄ crystals has been measured in the frequency range $f \sim 2\text{--}15$ GHz using a dielectric resonator technique. Z_s conforms to the classical skin effect only above 20 K, because the quasiparticle relaxation rate $1/\tau$ approaches $2\pi f$ at lower temperatures. Below T_c , R_s decreases while X_s initially increases and peaks at a frequency-dependent temperature. The microwave properties are quite unlike those of conventional and high- T_c superconductors and imply a finite quasiparticle fraction at $T=0$ with a temperature-independent relaxation time throughout the superconducting state.

DOI: [10.1103/PhysRevB.74.092504](https://doi.org/10.1103/PhysRevB.74.092504)

PACS number(s): 74.70.Pq, 07.57.-c, 74.20.De

The discovery of superconductivity in the copper-free layered perovskite superconductor¹ Sr₂RuO₄ has led to many experimental and theoretical studies of the pairing state in this material.² Detailed Fermi surface (FS) measurements have established three nearly cylindrical sheets,³ of which the γ sheet has been suspected as primarily responsible for the superconductivity.⁴ Evidence for p -wave superconductivity is supported by the extreme sensitivity of T_c to nonmagnetic impurities,⁵ the constancy of the spin susceptibility,⁶ the onset of spontaneous magnetization below T_c ,⁷ a flux line lattice with square symmetry,⁸ and phase-sensitive measurements.⁹ The experimental results have suggested an equal spin pairing state with the \mathbf{d} vector oriented along the c axis of the Sr₂RuO₄ crystal structure with \mathbf{d} having the symmetry $(k_x \pm ik_y)\hat{z}$.¹⁰ In a two-dimensional system, p -wave pairing with $\mathbf{d} \parallel \hat{z}$ can result in either an order parameter with constant magnitude $\Delta(\phi) = \Delta_0$, or a state with line nodes with $\mathbf{d} = k_x \hat{z}$ and $\Delta(\phi) = \Delta_0 \cos(\phi)$, although the latter would be in conflict with the time-reversal symmetry breaking.⁷ Early measurements of the heat capacity indicate $C/T \sim \gamma T$ with no significant residual linear contribution,¹¹ which implies either line nodes or a very anisotropic order parameter for consistency with the NMR (Ref. 6) and muon spin rotation⁷ data. The presence of line nodes or an extremely anisotropic order parameter would imply for the London penetration depth $\lambda_L(T) \propto T$ at low temperatures. In contrast, a T^2 dependence in $\lambda_L(T)$ has been observed in ac experiments between 0.04 and 0.8 K.¹² We report microwave measurements on high-purity Sr₂RuO₄ single crystals, which are consistent with the ac results in the temperature range 0.1 to 20 K and provide additional information about quasiparticle (qp) relaxation time and the normal fraction.

The complex surface impedance $Z_s = R_s + iX_s = \sqrt{i\mu_0\omega/(\sigma' - i\sigma'')}$ is a sensitive probe of the superconducting state, as previously applied to the high-temperature cuprate superconductors.^{13–15} The surface resistance $R_s(T)$ reflects losses from unpaired charge carriers, while the surface reactance $X_s(T) = \mu_0\omega\lambda_{eff}(T)$ probes an *effective* penetration depth $\lambda_{eff}(T)$, which is a model-dependent function of the normal and superfluid densities, and the qp relaxation time τ .

We have measured the surface impedance of a number of

high-purity Sr₂RuO₄ single crystals prepared by a traveling-solvent floating-zone method.¹⁶ The high purity of the crystals can be judged from the high transition temperatures $T_c = 1.47$ K for sample 1 and 1.42 K for samples 2 and 3, which are close to values for the ultraclean limit.⁵ The plate-like crystals had typical dimensions of $\sim 1 \times 1 \times 0.03$ mm³, with the c axis perpendicular to the major faces. Microwave measurements have been made using a hollow dielectric resonator¹⁷ in the temperature range from 25 K down to ~ 0.1 K. The crystals were mounted on the end of a cylindrical 0.5-mm-diameter sapphire rod centered along the axis of a resonant dielectric cylinder. The rod was fixed to a copper heater block thermally linked to a pumped ³He reservoir and adiabatic stage. The resonator and the enclosing copper cavity were thermally linked to a pumped liquid ⁴He bath at 1.4 K. Application of a static magnetic field enabled measurements of the normal state at temperatures below T_c . Zero-field measurements were performed in the ambient laboratory magnetic field.

Microwave measurements were performed using the TE₀₁₁, TE₀₁₂, and TE₀₁₃ modes of sapphire, LaAlO₃, and rutile resonators with modes at resonant frequencies of $f_0 = 2.1, 4.5, 8.5, 10.2,$ and 15.0 GHz. For all modes, the microwave magnetic field component at the sample position was parallel to the axis of the sapphire rod and the c axis of the crystal. The induced currents therefore flow parallel to the RuO₂ planes. The microwave properties were independent of field strength for, at least, a 30-fold increase of the microwave field. The surface resistance and changes in surface reactance of the crystals were deduced from the full width at half maximum Δf_B and changes of f_0 of the dielectric resonator using the relation $\Delta f_B(T) - 2i\Delta f_0(T) = \Gamma_f(R_s + i\Delta X_s)$, where Γ_f is the mode-specific filling factor of the sample. Δf_B was corrected for contributions from the host resonator using reference measurements in the absence of the sample. Long-term frequency drifts were corrected by regularly monitoring f_0 at a fixed temperature, typically 0.6 K for low-temperature measurements. The sensitivity and reproducibility within a single run, $\Delta f_B \sim \Delta f_0 \sim 100$ Hz, enables us to measure temperature dependences of small samples at temperatures well below 1 K.

Figure 1 shows the variation of R_s (dots) and X_s (open

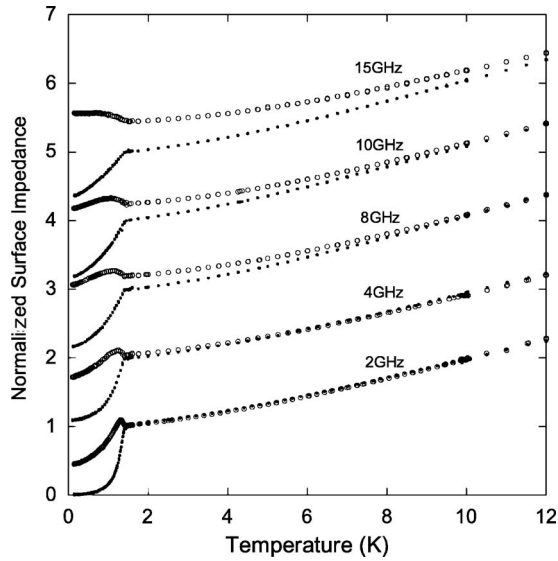


FIG. 1. Surface resistance (dots) and reactance (open circles) normalized to the surface resistance R_n at $T_c=1.47$ K for the Sr_2RuO_4 crystal 3 at 2, 4, 8, 10, and 15 GHz.

circles) over a wide temperature range for sample 3 at 2, 4, 8, 10, and 15 GHz. The data have been corrected for the background contributions from the resonator and scaled by the normal state surface resistance at T_c . Above 20 K, $X_s \approx R_s$ as expected for a normal metal in the low $\omega\tau \ll 1$ limit. Therefore, as changes in surface reactance can be measured, the $\Delta X_s(T)$ data have been shifted to match the surface resistance data above 20 K. The R_s and X_s data at 4, 8, 10, and 15 GHz have been offset by units of +1 for clarity.

Over most of the temperature range, the temperature-dependent changes of R_s and X_s are almost identical, as expected for the classical skin effect, $Z_{s0} = (1+i)[\mu_0\omega\rho_{dc}/2]^{1/2}$. In addition, the microwave data are found to be in excellent agreement with the published dc resistivity for samples with comparable purity in both the absolute value and temperature dependence, with $\rho_{dc} \sim 0.19 \mu\Omega \text{ cm}$.

Comparing the R_s and X_s data in Fig. 1, we find that R_s and X_s increasingly deviate at the higher frequencies. We associate this behavior with the increasing value of $\omega\tau(T)$. This leads to a normal state surface impedance $Z_s \sim (1+i\omega\tau)^{1/2} \times Z_{s0}$. We note that we have neglected possible complications from nonlocal effects in making an accurate fit to our data using this extended two-fluid Drude model. This suggests that such effects may not be a significant factor for $\omega\tau < 1$, as already implied by Hein *et al.*¹⁸

The low-temperature behavior indicated in Fig. 1 is illustrated in more detail in Fig. 2, where we have plotted R_s and ΔX_s at 2, 4, 8, 10, and 15 GHz for sample 3 in the normal state and the superconducting state from 1.5 K down to the lowest temperatures ~ 0.1 K. On entry to the superconducting state, the losses decrease as the qp's condense into pairs. In contrast, the reactance and hence the effective penetration depth λ_{eff} initially *increase*, rising to a frequency-dependent maximum well below T_c before decreasing toward its low-temperature value. Measurements on samples 1 and 2 exhibited essentially identical behavior.

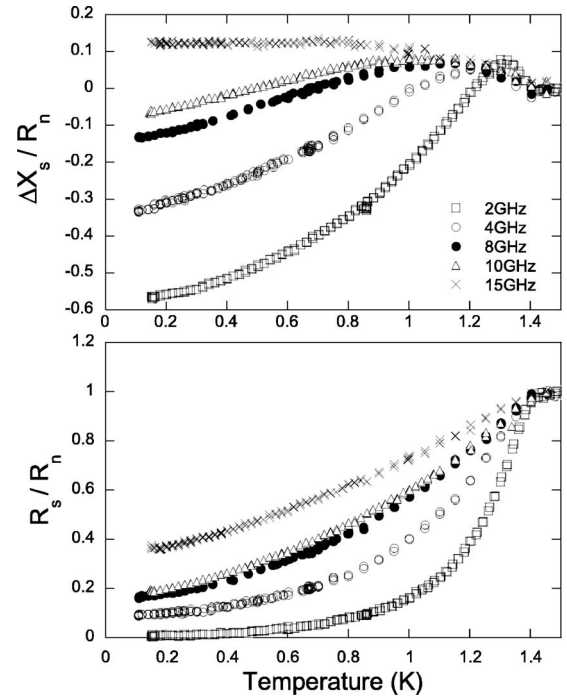


FIG. 2. Normalized surface reactance (top) and resistance (bottom) for the Sr_2RuO_4 crystal 3 at 2, 4, 8, 10, and 15 GHz.

The surface resistance and reactance can be analyzed using conventional methods to obtain the real and imaginary parts of the conductivity, shown in Fig. 3 at 2 GHz. The real part is seen to pass through a weak maximum and remain high even to the lowest temperatures. This is indicative of a large normal residual fraction even to the lowest temperatures, unlike the behavior of cuprates and conventional superconductors. The imaginary part rises at low temperatures and is not inconsistent with the T^2 dependence as observed in ac measurements.¹² We believe that the above behavior is intrinsic to this material and is irrespective of the surface

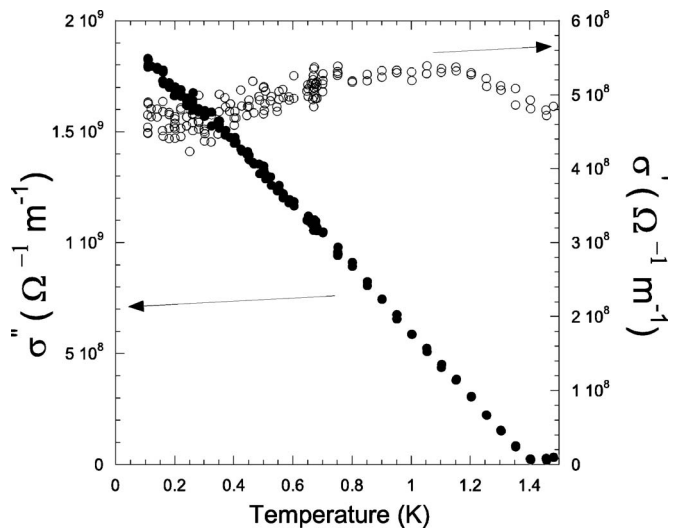


FIG. 3. The real and imaginary parts of the conductivity extracted from the measured surface impedance at 4 GHz assuming $R_s = X_s$ at T_c .

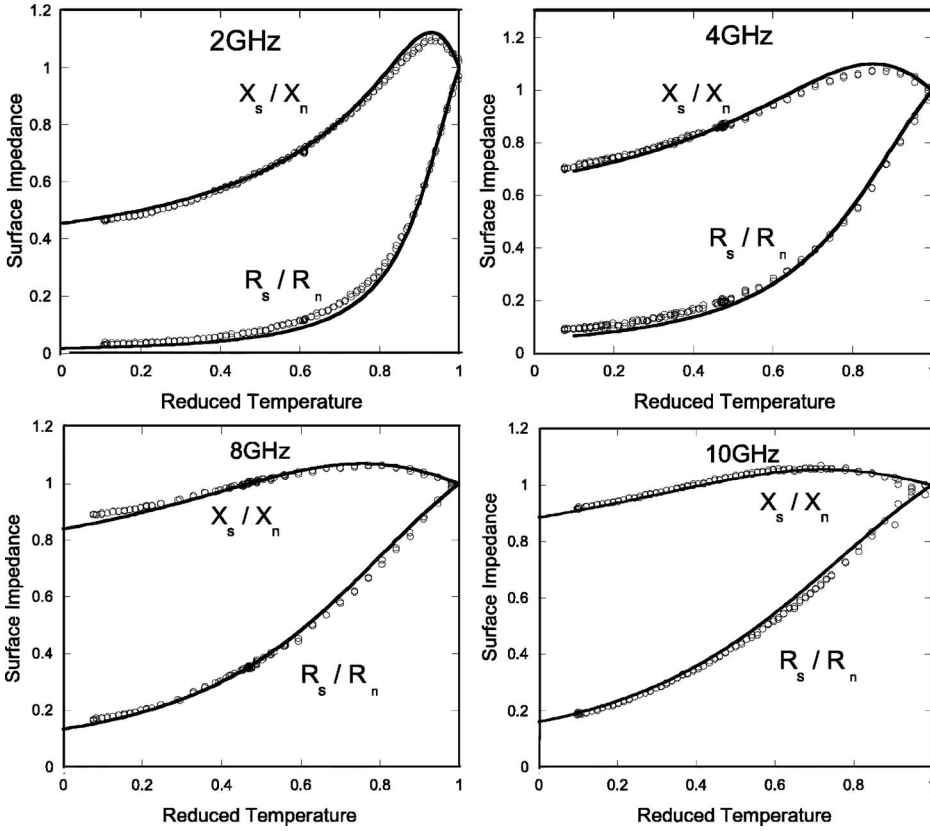


FIG. 4. The surface resistance and reactance at 2, 4, 8, and 10 GHz. Solid lines represent fits using the above model.

quality. The samples were subjected to an etching process to produce clean new surfaces and no measurable difference was obtained between the post- and pre-etched samples.

To describe our measurements of R_s and X_s at all frequencies, we have assumed that a fraction ε of the normal state electrons remain unpaired to the lowest temperatures. This leads to a modified two-fluid model, which includes a contribution from the unpaired electrons,

$$\sigma = \left[\left(\frac{f_N \tau_{qp}}{1 + i\omega \tau_{qp}} + \frac{f_S}{i\omega} \right) (1 - \varepsilon) + \frac{\tau_n}{(1 + i\omega \tau_n)} \varepsilon \right] \frac{1}{\mu_0 \lambda_0^2}, \quad (1)$$

where f_N and f_S are the normal and superfluid fractions, with $f_S + f_N = 1$ and $\mu_0 \lambda_0^2 = m/n e^2$. We also allow for a possible difference between the qp relaxation time τ_{qp} and the normal electron relaxation time τ_n . The values of the effective qp density n and effective mass m can, in principle, be determined from the known FS properties,³ depending on the relative contributions of the three sheets to the electronic transport. Below T_c , τ_n is assumed to follow the same temperature dependence as above T_c .

Using the above expression, we can fit both the surface resistance and reactance at all the measured frequencies with a single set of fitting parameters, ε , $f_S(T)$, λ_0 , and importantly $\tau_{qp} = \tau_n$. This is shown in detail by the solid curves through the experimental points in Fig. 4.

We immediately note that the temperature dependences of R_s , X_s , and τ_{qp} are quite unlike that of the cuprate d -wave superconductors or indeed of conventional s -wave superconductors, in particular τ_{qp} is temperature independent.^{19,20} There is no dramatic decrease in the surface resistance on

entering the superconducting state, which arises in most superconductors from the much reduced penetration of microwave fields at the surface. There is also a marked increase in penetration followed by a peak in the surface reactance below T_c , which moves to lower temperatures on increasing frequency. This corresponds to an increase in the microwave penetration depth on entering the superconducting state. Such a peak is predicted by the two-fluid model (see, for example, Ref. 18). It arises because, on entering the superconducting state, the initial reduction in normal electrons leads to an initial reduction in screening of the microwave field, with the increase in superconducting current in phase quadrature having little immediate effect. The peak in X_s occurs when $f_S \sim \omega \tau / 2$, which is too close to T_c in the cuprate superconductors below ~ 100 GHz. In Sr_2RuO_4 , the peak dominates the temperature dependence of X_s below T_c , because the low-temperature electron mean free path and qp relaxation time are so large. We note that the form used to fit the experimental data in Fig. 4 fails to reproduce the slight peak in $\sigma'(T)$. Even better agreement could be obtained by allowing τ_{qp} to be temperature dependent. However, in the absence of any microscopic theory we hesitate in further complicating our model.

For all the crystals where detailed measurements were undertaken the measured data are extremely well described over the whole superconducting temperature range at all frequencies using $\varepsilon = 0.22$, $\lambda_0 = 1600 \text{ \AA}$, and $\tau_n \sim 4$ ps. The derived value of the lifetime gives $\rho_{dc}(T_c) \sim 0.1 \mu\Omega \text{ cm}$, depending on the assumptions made about the contributing FS sheets.^{3,8} This value agrees well with the resistivity derived from the normal state surface resistance.

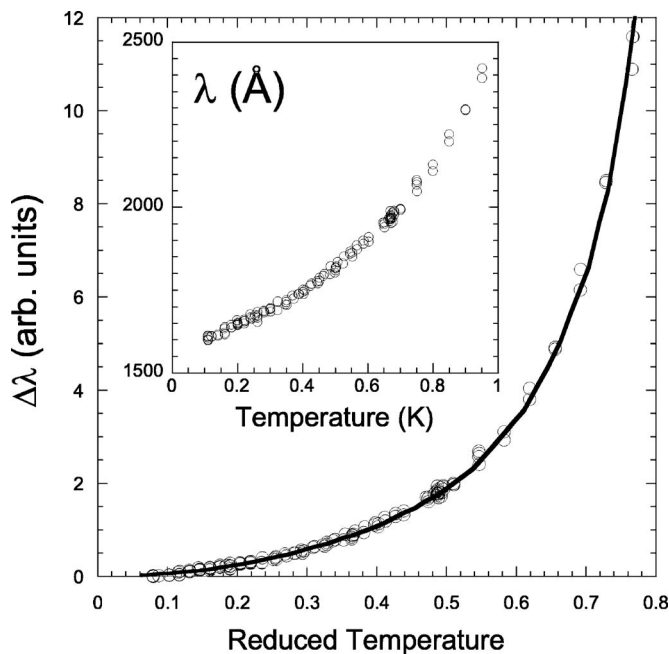


FIG. 5. The change in penetration depth extracted from the 2 GHz data. The solid line represents low-frequency data obtained by Bonalde *et al.* (Ref. 12). The inset shows the low-temperature region of $\lambda(T)$.

$\lambda(T)$ is shown in Fig. 5, extracted from the 2 GHz data. Also included are the 28 MHz data for comparison as a solid line.¹² We note the excellent agreement between two measurements at very different frequencies and the quadratic temperature dependence of λ , which has been taken to indicate the presence of low-lying excitations.

The residual losses at low temperatures could arise from unpaired charge carriers in the α and β sheets of the FS.⁴ This is inconsistent with early heat capacity measurements,¹¹ in which C/T appears to decrease to zero. However, the most recent heat capacity measurements do indeed show a nonzero intercept in C/T .²¹ In addition, recent scanning tunnel microscope measurements have suggested that there is a large off-

set in the qp spectrum of the superconducting order parameter of Sr_2RuO_4 .²²

Alternatively, residual losses could arise from Andreev reflection or diffuse scattering at the surfaces, modifying the p -wave order parameter within a distance of the coherence length ξ_{ab} from the edges of the crystal.²³ This could be an important effect in our experimental configuration since ξ_{ab} is only slightly smaller than the London penetration depth.⁸ We can also consider the possibility of pair breaking by the microwave field, when $\hbar\omega$ exceeds the order parameter in regions of small gap values due to nodes or strong gap anisotropy.²⁴ This might result in residual losses $x_N(0) \sim (\hbar\omega/\Delta_0) \sim 0.02-0.1$ at 10 GHz, depending on whether one assumes the BCS weak coupling result $\Delta_0 = 1.76kT_c$ or $\Delta_0 \sim 1$ meV suggested by tunneling measurements.²⁵

In summary, we report detailed measurements of the surface impedance of a number of high-purity Sr_2RuO_4 crystals at 2, 4, 8, 10, and 15 GHz in the normal and superconducting states from well above to well below T_c . In the normal state well above T_c , the data are well described by the classical skin effect with equal surface resistance and reactance determined by the strongly temperature-dependent dc resistivity. The high purity of the Sr_2RuO_4 crystals leads to $\omega\tau \sim 1$ at $T \sim T_c$, resulting in significant deviations from the classical limit. In the superconducting state, the losses decrease monotonically, while the effective penetration depth initially increases and passes through a frequency-dependent peak well below T_c . This behavior can be described by a two-fluid model with a Drude-like qp conductivity with finite and temperature-independent τ . In addition, to account for what we believe to be intrinsic residual losses, we have to assume that a fraction of electrons remain unpaired at low temperatures. The derived London penetration depth displays a quadratic temperature dependence consistent with the results of ac measurements.

We are grateful to E. M. Forgan, P. G. Kealey, and A. P. Mackenzie for valuable discussions, and to D. Brewster and G. Walsh for technical support. M.A.H. thanks the EPSRC and the Land Nordrhein-Westfalen (Germany) for financial support. This research has been funded by the EPSRC of the United Kingdom.

*Present address: Department for RF and Microwave Techniques, Technical University of Ilmenau, P.O. Box 10 05 65, 98684 Ilmenau, Germany.

¹Y. Maeno *et al.*, *Nature (London)* **372**, 532 (1994).
²A. P. Mackenzie and Y. Maeno, *Rev. Mod. Phys.* **75**, 657 (2003).
³A. P. Mackenzie *et al.*, *Phys. Rev. Lett.* **76**, 3786 (1996).
⁴D. F. Agterberg *et al.*, *Phys. Rev. Lett.* **78**, 3374 (1997).
⁵A. P. Mackenzie *et al.*, *Phys. Rev. Lett.* **80**, 161 (1998).
⁶K. Ishida *et al.*, *Nature (London)* **396**, 658 (1998).
⁷G. M. Luke *et al.*, *Nature (London)* **394**, 558 (1998).
⁸T. M. Riseman *et al.*, *Nature (London)* **396**, 242 (1998); **404**, 629 (2000).
⁹K. D. Nelson *et al.*, *Science* **306**, 1151 (2004).
¹⁰A. P. Mackenzie and Y. Maeno, *Physica B* **280**, 148 (2000).
¹¹S. Nishizaki *et al.*, *J. Phys. Soc. Jpn.* **69**, 572 (2000).
¹²I. Bonalde *et al.*, *Phys. Rev. Lett.* **85**, 4775 (2000).
¹³J. P. Carbotte, *Rev. Mod. Phys.* **62**, 1027 (1990).

¹⁴V. Krezin *et al.*, *Mechanisms of Conventional and High- T_c Superconductivity* (Oxford University Press, New York, 1993).
¹⁵D. A. Bonn *et al.*, *Phys. Rev. B* **47**, 11314 (1993).
¹⁶Z. Q. Mao *et al.*, *Mater. Res. Bull.* **35**, 1813 (2000).
¹⁷J. J. Wingfield *et al.*, *IEEE Trans. Appl. Supercond.* **7**, 2009 (1997).
¹⁸H. J. Fink, *Phys. Rev. B* **61**, 6346 (2000); M. A. Hein *et al.*, *Phys. Rev. B* **64**, 024529 (2001).
¹⁹S. M. Quinlan *et al.*, *Phys. Rev. B* **49**, 1470 (1994).
²⁰A. Hosseini *et al.*, *Phys. Rev. B* **60**, 1349 (1999).
²¹K. Deguchi *et al.*, *Phys. Rev. Lett.* **92**, 047002 (2004).
²²C. Lupien *et al.*, *cond-mat/0503317* (unpublished).
²³M. Matsumoto and M. Sigrist, *J. Phys. Soc. Jpn.* **68**, 994 (1999); **68**, 3120(E) (1999).
²⁴K. Miyake and O. Narikiyo, *Phys. Rev. Lett.* **83**, 1423 (1999).
²⁵F. Laube *et al.*, *Phys. Rev. Lett.* **84**, 1595 (2000).